Report on the 2004 SCEC proposal: "Testing for Stress Shadows"

Karen Felzer Emily Brodsky

November 19, 2004

1 Summary

A fundamental question in earthquake physics is whether aftershocks are predominantly triggered by static stresses (permanent stress changes associated with fault displacement) or dynamic stresses (temporary stress changes associated with earthquake shaking). Only the static stress model predicts stress shadows, or regions in which activity is decreased by a nearby earthquake. In our 2004 SCEC proposal we proposed to test whether static or dynamic stresses were most important for aftershock triggering by investigating whether stress shadows occur. We have found that there is no evidence for stress shadows following the 1983 $M6.5$ Coalinga, 1989 M 7.0 Loma Prieta, and 1994 $M6.7$ Northridge earthquakes. There is a region of reduced seismicity following the 1992 $M7.3$ Landers earthquake, but it does not cover the whole area where a stress shadow is expected. We also investigated the 1906 San Francisco earthquake. We find that the lower time-averaged rate of seismicity after this earthquake might be more readily explained by the continuous decay of aftershocks of the 1857 Ft. Tejon earthquake than by the stress shadow model.

We have submitted a paper on this work to the Journal of Geophysical Research. This work has also been orally presented at the 2004 RELM meeting in Lake Arrowhead, at the 2004 annual meeting of the Seismological Society of America, at the the 2004 annual SCEC meeting, at the USGS/Menlo Park, and at USC. This work is applicable to the SCEC 2004 RFP Interdisciplinary Focus Area 3, Earthquake Source Physics, and to SCEC 2004 RFP Interdisciplinary Focus Area 5, Seismic Hazard Analysis.

2 The test for stress shadows

To test for whether a stress shadow is present we look for a sudden seismicity rate decrease, coincident to the time of the mainshock, over the entire region in which a stress shadow is expected. Static stress change models may, in theory, be used to find the expected stress shadow region. But current stress shadow modeling is known to be imprecise for a number of reasons, including the unknown orientations of receiver faults (Kilb 2001), heterogeneous rock structures (Langenheim and Jachens 2002; Hearn et al. 2002), unknown details of mainshock rupture, and the effects of secondary aftershocks (Felzer et al. 2002). Thus we resort to an empirical method to find the expected stress shadow region. According to the static stress change model a mainshock should generate a region of stress increase, a region of neutral stress change, and a region of stress decrease. The region where stress has increased can be identified because it contains aftershocks. Once this region is identified and removed what is left should be dominated by stress shadow.

Our empirical method to find and eliminate aftershock regions uses a new statistic that we will call the time ratio, R. Unlike traditional declustering methods the time ratio does not attempt to remove all aftershocks of any earthquake from the data set, nor does it evaluate whether individual earthquakes are aftershocks. Instead it identifies spatial regions that contain at least some aftershocks of a particular mainshock. In simulation tests the time ratio misses aftershocks about 2.4% of the time.

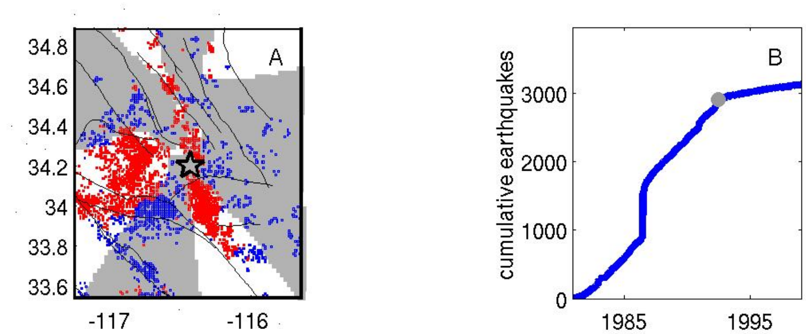

Figure 1: Test of the ability of the R statistic to identify a stress shadow in simulated data. A) Locations of the imposed and recovered stress shadow. Areas where stress was decreased in the simulation are shaded gray; stress was increased in the white areas. Boxes identified by the time ratio method as containing aftershocks are colored in red and boxes identified as not containing aftershocks are colored in blue. If the time ratio worked perfectly all of the boxes in the white area would be red, and all of the boxes in the gray area would be blue. B) Time series of the earthquakes in areas identified as not containing aftershocks by the time ratio. The simulated stress shadow is clearly recovered as a sudden seismicity rate decrease at the time of the mainshock (indicated by a gray dot).

2.1 The time ratio statistic

Our goal with the time ratio is to identify spatial subregions containing aftershocks of a particular mainshock occuring at time T_M. A seemingly simple way to determine whether a spatial bin contains aftershocks is to divide the rate of earthquakes after T_M in the bin by the rate beforehand, but this method runs the risk of producing false negatives if an active local aftershock sequence occurring before T_M overwhelms the number of T_M aftershocks. Alternatively we might identify a bin as containing aftershocks if it has any earthquakes between T_M and $T_M + \Delta t$. This method is akin to traditional declustering methods but runs the risk of false positives as not every earthquake during this time period is necessarily an aftershock of T_M.

To minimize these problems we have developed the time ratio statistc, R, which is defined as follows,

$$R = \frac{\Delta t_2}{\Delta T} \tag{1}$$

where $\Delta t_2 = T_2 - T_M$ equals the time between the mainshock and the first earthquake to follow it and $\Delta T = T_2 - T_1$ equals the time between the first earthquake to follow the mainshock and the last earthquake to precede it. A single value of the time ratio is calculated for each spatial bin. In general, aftershocks are present when $R << 1$. The time ratio avoids contamination from unrelated aftershock sequences occurring at different times by only using the earthquakes occurring immediately prior to and after the mainshock at T_M. Problems can occur, however, if a bin contains only late aftershocks, giving it a large time ratio even though aftershocks are present, or if a bin contains a small time ratio simply by chance. To minimize these problems the distribution of time ratio values in other bins within a 4 km radius areconsidered in deciding whether or not a particular bin contains aftershocks.

To determine whether the time ratio empirically isolates the area without aftershocks well enough to indicate a stress shadow if one existed we see if the time ratio can recover a realistic simulated stress shadow. We found that we can recover simulated stress shadows for the 1992 M_W7.3 Landers and 1992 M_W 6.1 Joshua Tree earthquakes (Figure 1).

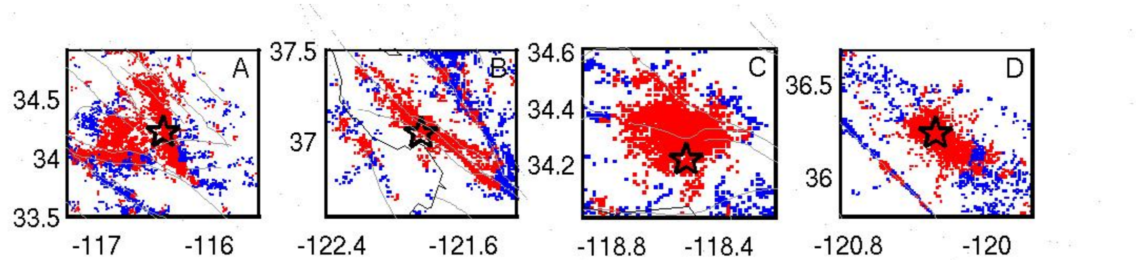

Figure 2: Maps showing spatial bins that were classified as containing aftershocks (red) and as not containing aftershocks (blue) of the (A) M 7.3 Landers earthquake, (B) M 7.0 Loma Prieta earthquake, (C) M 6.7 Northridge earthquake, and (D) M 6.5 Coalinga earthquake. The non-aftershock area of the Loma Prieta earthquake (B) includes the aftershock zones of the 1979 M 5.8 Coyote Lake earthquake, M 6.2 1984 Morgan Hill earthquake, and M 5.7 1986 Mt. Lewis earthquake.)

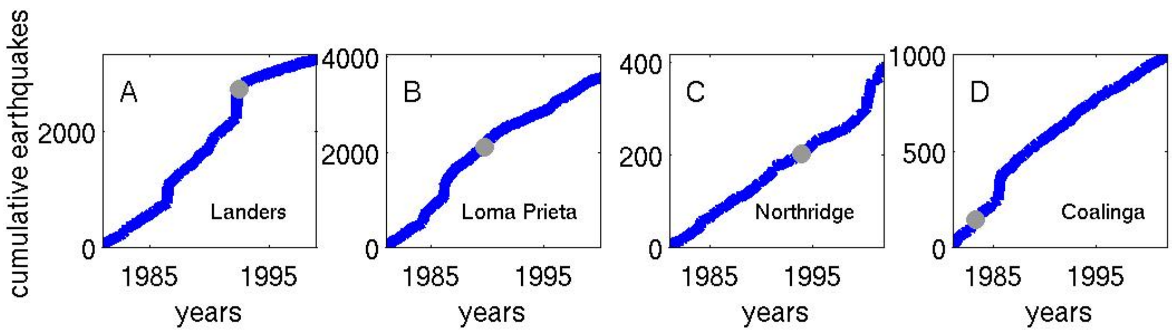

Figure 3: Time series of earthquakes in the region within 1.5 fault lengths of the mainshock that is classified as not containing aftershocks. If a stress shadow is present we expect a sudden decrease of the seismicity rate at the time of the mainshock. Gray dots indicate the time of the mainshock. (A) Time series for the Landers earthquake, $M > 2.0$ (we stop the time series before the nearby M 7.1 Hector Mine earthquake in October 1999. (B) Loma Prieta mainshock time series, $M > 1.5$. (C) Northridge mainshock time series, $M > 1.7$. (D) Coalinga time series, $M > 2.0$

3 Results

We use the time ratio statistic to classify spatial bins as either containing or not containing aftershocks of the 1983 $M6.7$ Coalinga, 1989 $M7.0$ Loma Prieta, 1992 $M7.3$ Landers, and 1994 $M6.7$ Northridge earthquakes. We plot maps of the areas classified as containing and not containing aftershocks for each mainshock, (Figure 2) and time series of all of the earthquakes locating in classified non-aftershock bins for each mainshock (Figure 3). The Coalinga, Loma Prieta, and Northridge earthquakes show no decrease in seismicity rate in the expected stress shadow region at the time of the mainshock. This suggests that these earthquakes did not produce stress shadows.

For the Landers earthquake there is a reduction in the seismicity rate when the time series is viewed over the long term. It is possible that what we are seeing in this case is a stress shadow. The downturn in the seismicity rate is not spread over the entire region in which a stress shadow is predicted, however, but instead is primarily localized to a region to the east of the main Landers aftershock zone and to the south of the future 1999 M 7.1 Hector Mine earthquake rupture (Figure 4). This localization agrees with the results

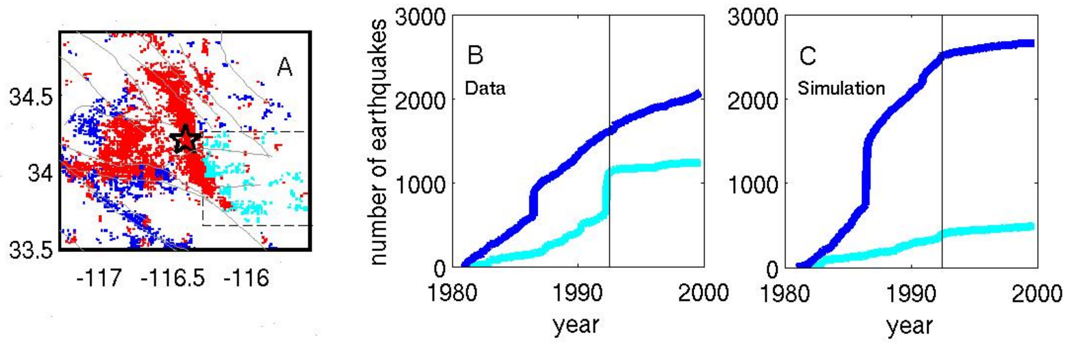

Figure 4: The majority of the downturn in rate at the time of the Landers earthquake is limited to a region in the southeast. (A) Red squares are regions classified as being aftershocks; blue squares are regions classified as containing aftershocks but not showing a shadow, and cyan squares are regions classified as being aftershocks and showing a seismicity rate decrease around the time of the Landers earthquake (B) The blue line gives time series of non-aftershocks in the blue squares; the cyan line the time series for non-aftershocks in the cyan squares. (C) Time series for simulated data in the blue and cyan regions, with an imposed shadow based on the stress changes calculated by Stein et al. (2004) and the rate and state equations of Dieterich (1994). According to this model an actual stress shadow should have caused a clear rate decrease in both of the non-aftershock regions.

of Marsan (2003), who found that there was an unusual degree of seismicity rate decrease in this region, but that earthquakes activity elsewhere in the predicted Landers stress shadow followed normal patterns of seismicity occurrence and aftershock decay.

4 San Francisco, 1906

A number of authors have proposed that the 1906 San Francisco earthquake caused a stress shadow that encompassed the entire Bay Area (Willis 1924; Ellsworth et al. 1981; Bufe and Varnes 1993; Jaume and Sykes 1996; Harris and Simpson 1998; Bakun 1999; Stein 1999). The argument for this shadow is that there were more earthquakes in the 50 to 75 years before 1906 than over the same period of time afterwards. The catalog by Bakun (1999) places the earthquake ratio for the fifty years before vs. the fifty years after 1906 for $M \geq 5.5$ earthquakes at about 5.5. The pre-1906 part of the catalog, however, which is based completely on historical data, contains much larger magnitude and location errors than the latter part of the catalog, creating a systematic bias that could create error in the ratio. The ratio also contains significant error from the fact that only $M > 5.5$ earthquakes can be used, limiting the size of the data set. We quantify part of this error by peforming Monte Carlo simulations in which we combine the magnitude errors given in Bakun (1999), the Gutenberg-Richter distribution (with a b value of 1.0) and Fisher's test for ratios. This gives us 95% confidence limits between 1.7 and 11.3 for the ratio of seismicity in the 50 years before vs. 50 years after 1906.

This results tells us that the seismicity rate decrease might have been relatively small, but definitely seems to have occurred. Was the decrease definitely caused by a stress shadow, however? It was noted by Bakun (2000) and Toppozada et al. (2002) that the average rate of $M > 5.5$ earthquakes didn't decrease only in the Bay Area but also to the south of the 1906 rupture. This is contrary to the static stress triggering model,

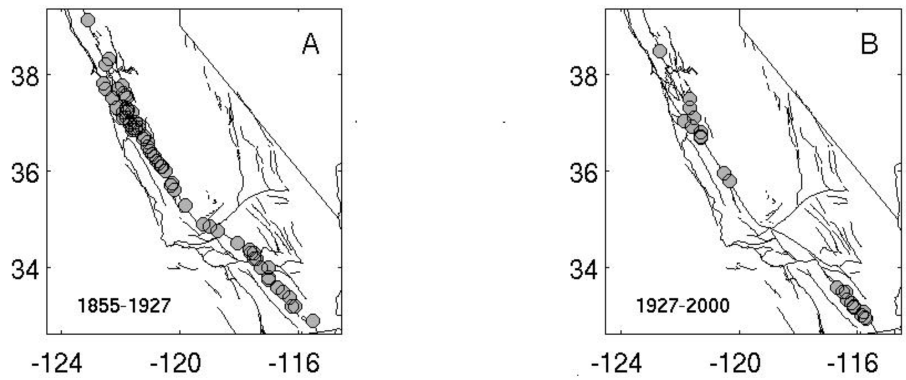

Figure 5: Large earthquakes along the entire San Andreas fault system have been less common in the last 75 years. (A) $M > 5.5$ earthquakes in from 1855-1927 within 15 km of the San Andreas, San Jacinto, and Hayward faults (B) $M > 5.5$ earthquaes 1927-2000. Data from California Geological Survey catalog, with historical earthquakes based on Toppozada et al. (2002).

which would predict a stress increase off the fault tip. To investigate this further we took the California Geological Survey catalog from 1855-2000 (which combines large historic and instrumental earthquakes) and compared the second half of the catalog (1927-2000) to the first half (1855-1927). We found a large decrease in seismicity along the entire extent of the fault system, from the Bay Area through Southern California Figure 5. Thus instead of a 1906 stress shadow we suggest that a system wide effect, such as errors in the historic catalog or the decay of aftershocks of the 1857 Ft. Tejon earthquake, are more likely explanations for the seismicity rate decrease.

5 Conclusions

Our work indicates that there is no clear evidence for stress shadows following the Coalinga, Loma Prieta, and Northridge earthquakes. A localized rate decrease did follow the Landers earthquake, but it only covered a fraction of the area that should have experienced a shadow. Our work also calls into question the existence of a stress shadow after the 1906 San Francisco earthquake. Although seismicity rates in the Bay Area were lower over the fifty years after 1906, the decrease in seismicity also extended south from the Bay Area along the San Andreas fault, through Southern California. This widespread decrease is inconsistent with a 1906-induced stress shadow and suggests instead that the whole pattern is a consequence of decaying aftershocks of the 1857 Ft. Tejon earthquake.

This lack of observable stress shadows suggests that aftershocks are dominantly triggered by dynamic rather than static stress changes.

References

Bakun, W. H. (1999). Seismic activity of the San Francisco Bay Region. *Bull. Seis. Soc. Am. 89*, 764–784.

Bakun, W. H. (2000). Seismicity of California's North Coast. *Bull. Seis. Soc. Am. 90*, 797–812.

Bufe, C. G. and D. J. Varnes (1993). Predictive modeling of the seismic cycle of the greater San Francisco Bay region. *J. Geophys. Res. 98*, 9871–9883.

Dieterich, J. A. (1994). Constitutive law for the rate of earthquake production and its application to earthquake clustering. *J. Geophys. Res. 99*, 2601–2618.

Ellsworth, W. L., A. G. Lindh, W. H. Prescott, and D. G. Herd (1981). *The 1906 San Francisco earthquake and the seismic cycle*, pp. vol. 4. Washington D.C.

Felzer, K. R., T. W. Becker, R. E. Abercrombie, Göran Ekström, and J. R. Rice (2002). Triggering of the 1999 $M_W 7.1$ Hector Mine earthquake by aftershocks of the 1992 $M_W 7.3$ Landers earthquake. *J. Geophys. Res. 107*, 2190, doi:10.1029/2001JB000911.

Harris, R. A. and R. W. Simpson (1998). Suppression of large earthquakes by stress shadows: A comparison of Coulomb and rate-and-state failure. *J. Geophys. Res. 103*, 24439–24451.

Hearn, E. H., R. Bürgman, and R. E. Reilinger (2002). Dynamics of Izmit earthquake postseismic deformation and loading of the Dücze earthquake hypocenter. *Bull. Seis. Soc. Am. 92*, 172–193.

Jaume, S. C. and L. R. Sykes (1996). Evolution of moderate seismicity in the San Francisco Bay region, 1850 to 1993: Seismicity changes related to the occurrence of large and great earthquakes. *J. Geophys. Res. 101*, 765–789.

Kilb, D. (2001). Fault parameter constraints using relocated earthquakes:implications for stress change calculations. Volume 82, pp. Abstract S11C–10.

Langenheim, V. E. and R. C. Jachens (2002). The Emerson lake body; a link between the Landers and Hector Mine earthquakes, Southern California, as inferred from gravity and magnetic anomalies. *Bull. Seis. Soc. Am. 92*, 1606–1620.

Marsan, D. (2003). Triggering of seismicity at short time scales following California earthquakes. *J. Geophys. Res. 108*, 2266,doi:10.1029/2002JB001946.

Stein, R. S. (1999). The role of stress transfer in earthquake occurrence. *Nature 402*, 605–609.

Stein, R. S., K. Richards-Dinger, S. Today, S. Bozkurt, and T. Dewez (2004). Rate/state forecast animations of seismicity from earthquake stress changes in southern California. in preparation.

Toppozada, T. R., D. M. Branum, M. S. Reichle, and C. L. Hallstrom (2002). San Andreas fault zone, California: $m \geq 5.5$ earthquake history. *Bull. Seis. Soc. Am. 92*, 2555–2601.

Willis, B. (1924). Earthquake risk in California. *Bull. Seis. Soc. Am. 14*, 9–25.